Trafficking-dependent phosphorylation of Kv1.2 regulates voltage-gated potassium channel cell surface expression

Jae-Won Yang*, Helene Vacher*, Kang-Sik Park*, Eliana Clark*, and James S. Trimmer*†‡

*Section of Neurobiology, Physiology, and Behavior, College of Biological Sciences; and †Department of Physiology and Membrane Biology, School of Medicine, University of California, Davis, CA 95616

Edited by David E. Clapham, Harvard Medical School, Boston, MA, and approved October 22, 2007 (received for review September 10, 2007)

Kv1.2 α-subunits are components of low-threshold, rapidly activating voltage-gated potassium (Kv) channels in mammalian neurons. Expression and localization of Kv channels is regulated by trafficking signals encoded in their primary structure. Kv1.2 is unique in lacking strong trafficking signals and in exhibiting dramatic cell-specific differences in trafficking, which is suggestive of conditional trafficking signals. Here we show that a cluster of cytoplasmic C-terminal phosphorylation sites regulates Kv1.2 trafficking. Using tandem MS to analyze Kv1.2 purified from rat, human, and mouse brain, we identified in each sample *in vivo* phosphoserine (pS) phosphorylation sites at pS434, pS440, and pS441, as well as doubly phosphorylated pS440/pS441. We also found these sites, as well as pS449, on recombinant Kv1.2 expressed in heterologous cells. We found that phosphorylation at pS440/pS441 is present only on the post-endoplasmic reticulum (ER)/cell surface pool of Kv1.2 and is not detectable on newly synthesized and ER-localized Kv1.2, on which we did observe pS449 phosphorylation. Elimination of PS440/PS441 phosphorylation by mutation reduces cell-surface expression efficiency and functional expression of homomeric Kv1.2 channels. Interestingly, mutation of S449 reduces phosphorylation at pS440/pS441 and also decreases Kv1.2 cell-surface expression efficiency and functional expression. These mutations also suppress trafficking of Kv1.2/Kv1.4 heteromeric channels, suggesting that incorporation of Kv1.2 into heteromeric complexes confers conditional phosphorylation-dependent trafficking to diverse Kv channel complexes. These data support Kv1.2 phosphorylation at these clustered C-terminal sites as playing an important role in regulating trafficking of Kv1.2-containing Kv channels.

ion channel | mass spectrometry | proteomics | brain | phosphospecific

Voltage-gated potassium, or Kv, channels that form as tetramers of Kv1 α-subunits play important and diverse roles in regulating excitability of axons, nerve terminals, and dendrites of mammalian neurons (1). The major Kv1 α-subunits in mammalian brain, Kv1.1, Kv1.2, and Kv1.4, are found predominantly in heterotetrameric channel complexes (2–4). Homotetrameric Kv1.2 channels form low-threshold, sustained- or delayed-rectifier Kv channels (5) and, when coassembled with other Kv1 α-subunits, can generate a diverse array of channel subtypes (6). In mammalian brain, Kv1.2 is found prominently along unmyelinated axons, in nerve terminals and/or in preterminal axon segments, at axon initial segments, and at juxtaparanodes of myelinated axons, but it is also present in the dendrites of some neurons (7). The physiological importance of Kv1.2 is underscored by the recent finding that Kv1.2 knockout mice have enhanced seizure susceptibility and die in the third postnatal week (8).

Biosynthetic trafficking of Kv1 channels from their site of translation in the rough endoplasmic reticulum (ER) to the cell surface is governed by a set of intrinsic targeting motifs encoded in primary structure and that differ among different Kv1 α-subunits (9). These include extracellular/luminal ER retention signals (10) and cytoplasmic C-terminal anterograde signals (11). These trafficking signals result in Kv1.1 homomers being predominantly retained intracellularly and in Kv1.4 homomers being efficiently trafficked to the cell surface (12). Coassembly of Kv1.1 and Kv1.4 into heterotetrameric channel complexes with different subunit composition yields different patterns of subcellular localization, consistent with dose-dependent effects of the trafficking signals present on the component subunits (12).

Kv1.2 α subunits are unique among Kv1 α-subunits in lacking strong retrograde (10) and anterograde (11) trafficking signals, such that homotetrameric Kv1.2 channels exhibit highly variable trafficking characteristics heavily influenced by other coexpressed Kv1 α- (12) and auxiliary Kvβ- (13–15) subunits. Kv1.2 trafficking also differs between different cells in a population (12, 14) and between different cell types (12). These characteristics suggest conditional regulation of Kv1.2 trafficking, as can occur upon changes in protein phosphorylation state as recently shown for the KCNK3 potassium channel (16). To better understand mechanisms that regulate the conditional trafficking of Kv1.2, here we undertook a proteomic analysis of Kv1.2 phosphorylation in mammalian brain *in vivo* and then investigated the role of this phosphorylation in trafficking of Kv1.2-containing Kv channels.

Results

Kv1.2 Is Phosphorylated in Brain and in Heterologous Cells. The Kv1.2 α-subunit contains a single N-linked oligosaccharide chain on the extracellular linker between the first and second transmembrane segments (17). On SDS gels, the Kv1.2 protein pool exists in two predominant forms (Fig. 1*A*); a form with a high Man oligosaccharide chain present at M_r = 57 kDa, and a form with a processed/complex oligosaccharide chain present at M_r = 78 kDa in brain and M_r = 73 kDa in heterologous cells (Fig. 1*A*) (17). The low M_r form corresponds to the newly synthesized ER-localized pool of Kv1.2, whereas the high M_r form is found in the Golgi apparatus and on the cell surface (12, 13). Because virtually all of the low and high M_r forms are in the ER and on the cell surface, respectively (12), for simplicity we will refer to the two pools hereafter as "ER" and "cell surface."

As a first step toward characterizing Kv1.2 phosphorylation, we subjected endogenous Kv1.2 in crude rat brain membranes (RBM) and recombinant rat Kv1.2 expressed in HEK293 cells to digestion with alkaline phosphatase (AP). Kv1.2 was expressed in HEK293

Author contributions: J.-W.Y. and H.V. contributed equally to this work; J.-W.Y., H.V., E.C., and J.S.T. designed research; J.-W.Y., H.V., and E.C. performed research; K.-S.P. contributed new reagents/analytic tools; J.-W.Y., H.V., K.-S.P., and J.S.T. analyzed data; and J.-W.Y., H.V., and J.S.T. wrote the paper.

The authors declare no conflict of interest.

This article is a PNAS Direct Submission.

‡To whom correspondence should be addressed at: Section of Neurobiology, Physiology, and Behavior, College of Biological Sciences, 196 Briggs Hall, University of California, One Shields Avenue, Davis, CA 95616-8519. E-mail: jtrimmer@ucdavis.edu.

This article contains supporting information online at www.pnas.org/cgi/content/full/0708574104/DC1.

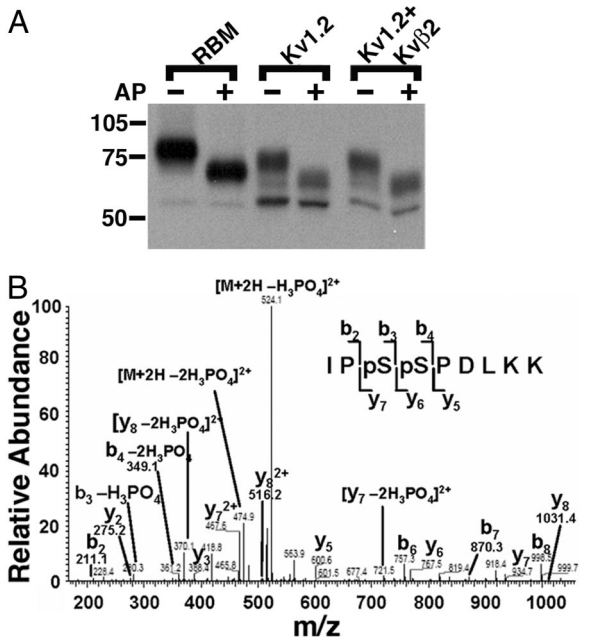

Fig. 1. Kv1.2 phosphorylation in mammalian brain and heterologous cells. (*A*) RBM and lysates from cells expressing Kv1.2 alone or Kv1.2 plus Kvβ2 were digested without (−) or with (+) AP, subjected to SDS/PAGE, and immunoblotted using a general Kv1.2-specific mAb (K14/16). Numbers on the left refer to molecular weight of prestained molecular weight standards. (*B*) Identification of phosphorylation sites on Kv1.2 in rat brain using LC-MS/MS. A doubly charged, doubly phosphorylated peptide at *m/z* 573.035, derived from Kv1.2 purified from rat brain, was fragmented to produce this MS/MS with y- and b-ion series that described the sequence IPpSpSPDLKK (amino acids 438–446). The phosphorylation sites were unambiguously assigned to S440 and S441 because of mass assignments from β-eliminated y6, y7, *b*3, and *b*4 fragment ions with neutral loss of phosphoric acid H_3PO_4 and $2H_3PO_4$.

cells without and with auxiliary Kvβ2 subunits to alter the relative proportions of ER and cell-surface pools (13–15). The high M_r cell-surface form of both native brain Kv1.2 and recombinant Kv1.2 from HEK293 cells underwent large shifts in M_r upon AP treatment (Fig. 1*A*), suggesting extensive phosphorylation. However, the low M_r ER form was not sensitive to AP digestion (Fig. 1*A*). These data suggest that Kv1.2 in brain and in heterologous cells is phosphorylated and that phosphorylation differs between ER and cell-surface Kv1.2 populations.

Liquid Chromatography–Tandem MS (LC-MS/MS) Identification of *in Vivo* Phosphorylation Sites on Kv1.2. To identify *in vivo* Kv1.2 phosphorylation sites, we undertook unbiased MS-based analyses of Kv1.2. We first purified Kv1.2 protein from RBM by immunoaffinity chromatography and size fractionation by SDS/PAGE. The Coomassie blue-stained band representing the high M_r form of Kv1.2 protein that predominates in adult rat brain (Fig. 1*A*) was excised and subjected to in-gel trypsin digestion. Kv1.2 peptides were identified using LC-MS/MS, and a Mascot database search of resultant mass spectra resulted in 289 matched peptides and 44% overall sequence coverage, representing 89% coverage of the cytoplasmic domains [supporting information (SI) Fig. 5]. This includes 96% coverage of the 160-aa cytoplasmic N terminus and 90% coverage of the 89-aa cytoplasmic C terminus. From these analyses, three phosphorylated amino acids were unambiguously identified (SI Fig. 6): phosphoserine (pS) 434 (ETEGEEQAQYLQVTpSCPK); pS440 (IPpSSPDLKK); and pS441 (IPSpSPDLKK). The peptide doubly phosphorylated at pS440/pS441 (IPpSpSPDLKK) was also identified (Fig. 1*B* and Table 1; see SI Fig. 7 for a higher gain view of low-abundance MS peaks). No other phosphorylated peptides were detected.

We next determined whether Kv1.2 was also phosphorylated in human brain. We purified Kv1.2 from crude human hippocampal and cerebellar membrane preparations, and, in both preparations, we unambiguously identified the singly phosphorylated peptides containing pS440 and pS441 and the doubly phosphorylated peptide at pS440/pS441 (Table 1 and SI Fig. 5). We also identified this same set of phosphorylation sites on Kv1.2 copurifying with Kv1.1 from mouse brain (Table 1 and SI Fig. 5); again, no additional phosphorylated peptides were detected. These data show a strong degree of conservation of Kv1.2 phosphorylation in rat, human, and mouse brain.

As a prelude to analyses of the impact of phosphorylation, we analyzed phosphorylation of recombinant rat Kv1.2 expressed in and purified from two mammalian kidney cell lines: HEK293 and COS-1. We found that recombinant rat Kv1.2 expressed in HEK293 cells was phosphorylated at the same exact set of sites that are phosphorylated in mammalian brain (pS434, pS440, pS441, pS440/pS441) as well as at an additional site, pS449 (SRpSASTISK; Table 1 and SI Fig. 5). Recombinant rat Kv1.2 expressed in COS-1 cells had detectable phosphorylation at three sites: pS440, pS441 and pS449 (Table 1 and SI Fig. 5). No other phosphorylated peptides were detected. As such, phosphorylation of Kv1.2 is similar on endogenous Kv1.2 in brain and recombinant Kv1.2 expressed in heterologous cells, with the exception of additional phosphorylation at pS449 found in the latter.

Differences in Phosphorylation Between ER and Cell-Surface Pools of Kv1.2. As shown in Fig. 1, the ER and cell-surface pools of Kv1.2 exhibit distinct sensitivities to AP digestion, suggesting differential phosphorylation. To better investigate the differences in phosphorylation between these two cellular Kv1.2 pools, we repeated the unbiased LC-MS/MS analysis on the separate high and low M_r forms of recombinant rat Kv1.2 expressed in HEK293 cells. We found an enhanced representation of doubly phosphorylated pS440/pS441 peptide in the high M_r cell-surface Kv1.2 pool, and we found no doubly phosphorylated peptides present in the low M_r ER pool by MS analyses (data not shown). pS449 was found in both ER and cell-surface samples, but pS449 was found more frequently in the former (data not shown).

To quantify levels of phosphorylated Kv1.2, we used stable isotope labeling with amino acids in cell culture (SILAC) (18, 19). We metabolically labeled HEK293 cells transiently transfected with

Table 1. MS identification of phosphorylation sites on Kv1.2 purified from brain or heterologous cells

	Native					Heterologous cells	
Phosphorylation site	Rat brain	Rat HC	Mouse brain	Human HC	Human CB	HEK293	COS-1
pS434	+	+	+	−	−	+	−
pS440	+	+	+	−	+	+	+
pS441	+	−	+	+	−	+	+
pS440/pS441	+	+	+	+	+	+	−
pS449	−	−	−	−	−	+	+

HC, hippocampus; CB, cerebellum; +, identified phosphorylation site; −, phosphorylation site not identified.

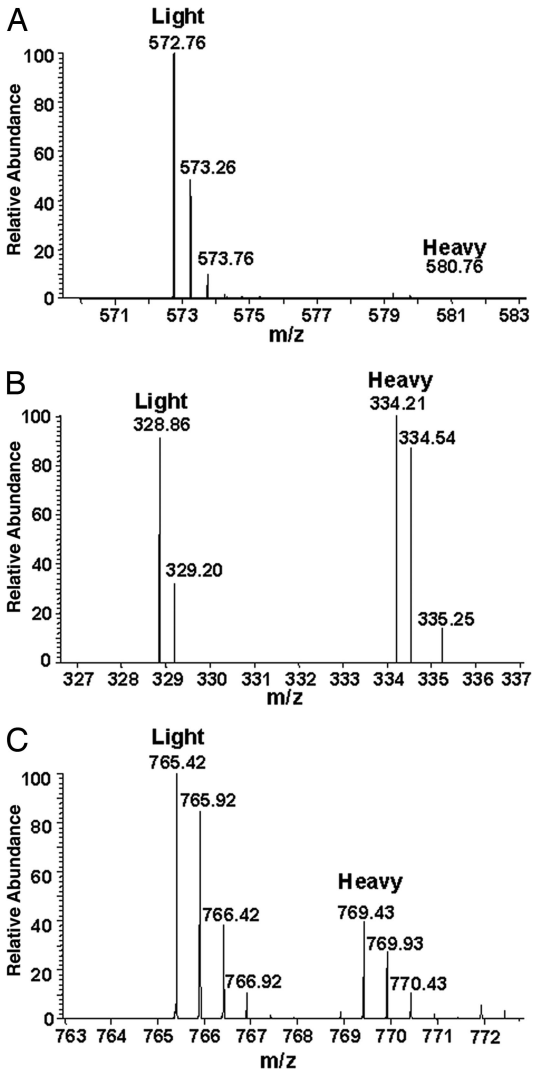

Fig. 2. Relative SILAC quantification of phosphorylated peptides between ER and cell-surface forms of Kv1.2. (*A*) A doubly charged peptide representing doubly phosphorylated Kv1.2 at pS440/pS441 (IPpSpSPDLKK) was abundant in the sample from the cell-surface Kv1.2 pool (Light, peak at *m/z* 572.76) but was not detected in the samples from the ER Kv1.2 pool (Heavy, lack of peak at *m/z* 580.76). (*B*) The corresponding triply charged unphosphorylated peptide (IPSSPDLKK) was found with similar mass peak intensities in both the cell surface (Light, peak at *m/z* 328.86) and ER (Heavy, peak at 334.21) Kv1.2 pools. (*C*) A representative doubly charged nonphosphopeptide (TLAQFPETLLGDPK) from Kv1.2 demonstrates the overall ratio (≈2:1) of Kv1.2 between cell surface (Light, peak at *m/z* 765.42) and ER (Heavy, peak at *m/z* 769.43) samples applied for SILAC analysis.

rat Kv1.2 and Kvβ2 with media containing naturally occurring Arg-0, Lys-0 amino acids, or their heavy stable isotopic counterparts, Arg-6 and Lys-8. Kv1.2 was immunopurified from the metabolically labeled cells, equal amounts of purified Kv1.2 were size-fractionated by SDS/PAGE, and high and low M_r forms of Kv1.2 were separately isolated from the Arg0Lys0- and Arg6Lys8-labeled samples. Aliquots of these samples (Arg0Lys0 high M_r band and Arg6Lys8 low M_r band, and vice versa) were then mixed, in-gel trypsin digested, and analyzed by LC-MS/MS using the stable isotope-conferred mass tag to distinguish Kv1.2 derived from the different gel bands.

As predicted from our preliminary qualitative analyses, the doubly phosphorylated pS440/pS441 peptide was only detected in the high M_r cell-surface form of Kv1.2 (Fig. 2*A*). The singly phosphorylated pS440 and pS441 peptides were enriched in the cell-surface pool and depleted in the ER pool. Conversely, the unphosphorylated form of this tryptic peptide, although found in both the high and low M_r forms of Kv1.2, was significantly enriched in the ER pool (Fig. 2*B*). Phosphorylation at pS449 could not be quantified because of technical difficulties.

Localization of Kv1.2 Phosphorylated at pS440/pS441 to the Cell Surface. To better study the Kv1.2 pool phosphorylated at pS440/pS441, we generated a rabbit polyclonal Ab against the doubly phosphorylated synthetic peptide CPKIPpSpSPDLKK. A two-step immunoaffinity purification procedure involving phosphopeptide enrichment and dephosphopeptide depletion yielded an Ab ("Kv1.2P") that displayed an ≈250-fold preference for binding to phospho- versus dephosphopeptide by ELISA (data not shown). On immunoblots, Kv1.2P recognized WT recombinant Kv1.2 expressed in HEK293 cells, but not the double phosphorylation site mutant S440A/S441A or either single phosphorylation site mutant, S440A and S441A (Fig. 3*A*). Interestingly, Kv1.2P immunoreactivity was greatly decreased in the S449A mutant, suggesting that phosphorylation at this site may be a prerequisite to that occurring at pS440/pS441 (Fig. 3*A*). In contrast, the S434A mutation did not impact Kv1.2P immunoreactivity (Fig. 3*A*). Consistent with our MS analyses, the Kv1.2P Ab only recognized the M_r = 73-kDa form of WT Kv1.2 expressed in HEK293 cells, and not the low M_r = 57-kDa form, nor an intermediate form at M_r = 64 kDa, which was present in this experiment (Fig. 3*A*). We also generated a mouse mAb (L64/4) from mice immunized with the same peptide that exhibited a similar pattern of immunoreactivity on immunoblots (data not shown).

Similar results were obtained in immunoprecipitation analyses, in which reactions performed with Kv1.2P yielded products from cells expressing WT Kv1.2, but not S440A/S441A (Fig. 3*B*), and only the M_r = 73-kDa form of WT Kv1.2 expressed in HEK293 cells was selectively immunoprecipitated by Kv1.2P, whereas an immunoprecipitation reaction performed with a general anti-Kv1.2 Ab yielded products proportional to their input levels (Fig. 3*C Left*). Kv1.2P was also effective at immunoprecipitating Kv1.2 from RBM (Fig. 3*C Center*). To confirm the cell-surface expression of pS440/pS441 on Kv1.2, we selectively labeled the cell-surface pool of Kv1.2 by cell-surface biotinylation. Analysis of the total, biotinylated cell surface (enriched by binding to streptavidin–agarose) and nonbiotinylated intracellular (unbound fraction from streptavidin–agarose) forms of Kv1.2 by immunoblot yielded detectable Kv1.2P immunoreactivity in the total cell lysate and biotinylated fraction, but not in the intracellular pool (Fig. 3*C Right*).

Double-label immunofluorescence staining of COS-1 cells expressing WT Kv1.2 with rabbit anti-Kv1.2P and the phospho-independent mouse mAb K14/16 showed strong staining of a subset of Kv1.2-expressing cells (Fig. 3*D Top*). The Kv1.2P-positive cells exhibited strong plasma membrane-associated Kv1.2P staining, with no obvious staining of the intracellular K14/16-associated pool present in those cells. Cells that exhibited only intracellular/perinuclear K14/16 staining in the absence of obvious plasma membrane-associated staining did not exhibit specific Kv1.2P staining (Fig. 3*D Top*). The staining pattern of Kv1.2P resembled that obtained when intact cells were stained with an ectodomain-directed Kv1.2e Ab (Fig. 3*D Middle*). To more definitively show that only cells expressing cell-surface Kv1.2 exhibited phospho-specific Ab staining, we stained intact cells with Kv1.2e, followed by permeabilization and staining with the Kv1.2P-specific mAb L64/4. We found that that all cells exhibiting Kv1.2e staining also exhibited robust staining for L64/4 (Fig. 3*D Bottom*). These immunofluorescence results, taken together with data from the LC-MS/MS, SILAC, and biochemical analyses described above, provide compelling evidence that phosphorylation at Kv1.2 pS440/pS441 is specific to the cell-surface Kv1.2 pool.

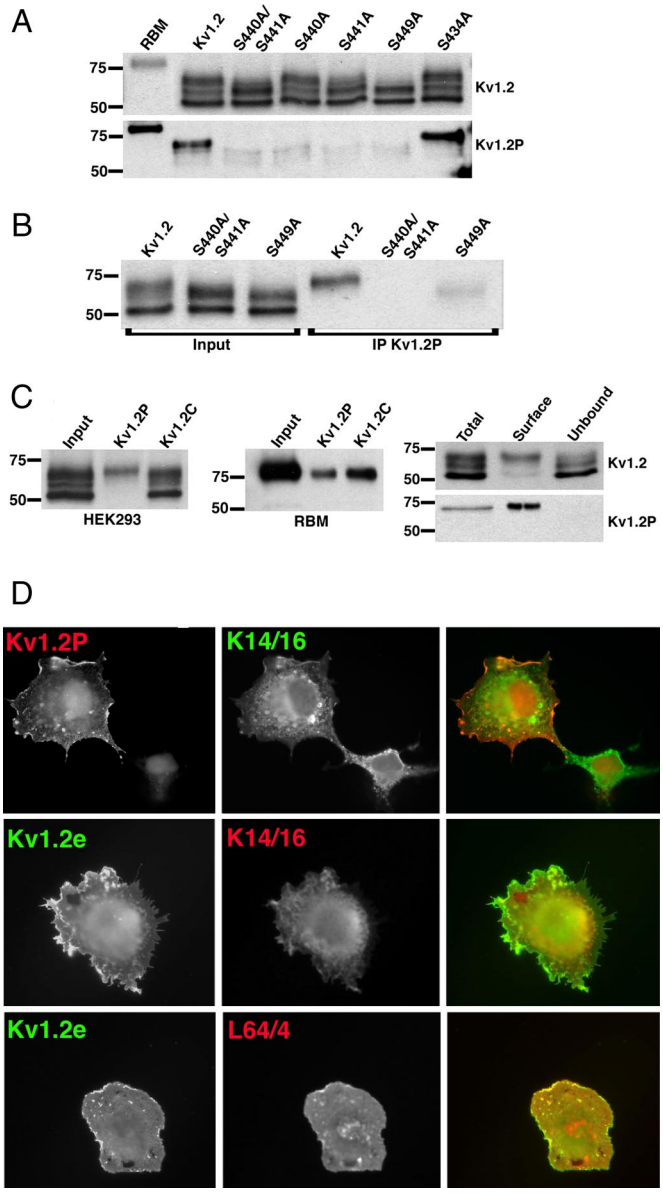

Fig. 3. Phosphospecific Abs Kv1.2P and L64/4 specifically recognize cell-surface Kv1.2. (*A*) Immunoblot analysis performed against RBM prepared from postnatal day 15 (P15) brain and lysates from HEK293 cells expressing WT Kv1.2 and phosphorylation site mutants S440A/S441A, S440A, S441A, S449A, and S434A. Shown is immunoreactivity using the general anti-Kv1.2 mAb K14/16 (*Upper*) and using the pS440/pS441-specific Kv1.2P rabbit Ab (*Lower*). (*B*) Input into and products of immunoprecipitation reactions performed with Kv1.2P Ab on lysates from HEK293 cells expressing WT Kv1.2, S440A/S441A, and S449A and blotted with K14/16. (*C*) (*Left*) Input into and products of immunoprecipitation reactions performed with Kv1.2P and Kv1.2C Abs on lysates from HEK293 cells expressing WT Kv1.2, and blotted with K14/16. (*Center*) Input into and products of immunoprecipitation reactions performed with Kv1.2P and Kv1.2C Abs on lysates of RBM as assessed by immunoblotting with K14/16 Ab. (*Right*) Cell surface biotinylated (Surface) and intracellular nonbiotinylated (Unbound) pools of WT Kv1.2 in HEK293 cells were isolated by surface biotinylation and streptavidin–agarose enrichment/depletion, respectively, from a total biotinylated cell lysate (Total). Fractions were immunoblotted for total Kv1.2 with K14/16 (*Upper*) and with Kv1.2P (*Lower*) Abs. Numbers on the left in all immunoblots refer to the molecular weight of prestained molecular weight standards. (*D*) COS-1 cells transfected with WT Kv1.2 were double immunofluorescence stained with K1.2P (red) and K14/16 (green) after permeabilization (*Top*), with Kv1.2e (green) before and K14/16 (red) after permeabilization (*Middle*), or Kv1.2e (green) before and L64/4 (red) after permeabilization (*Bottom*).

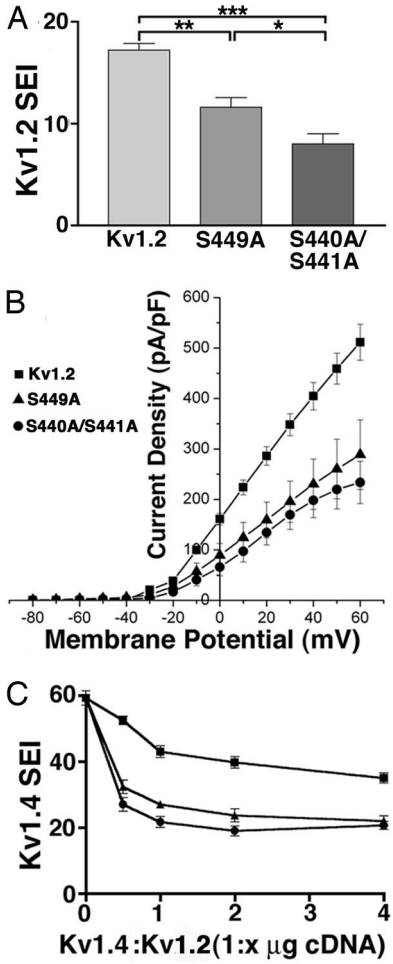

Fig. 4. Mutations at *in vivo* phosphorylation sites suppress Kv1.2 surface expression and Kv1.2 currents. (*A*) COS-1 cells transfected with WT Kv1.2, S440A/S441A, or S449A were double immunofluorescence stained with Kv1.2e before and K14/16 after permeabilization, and a SEI determined the percentage of Kv1.2-expressing (K14/16-positive) cells with Kv1.2e surface staining. Statistical significance was determined by one-way ANOVA followed by Turkey's post hoc test, and statistical significance was considered at *, $P < 0.05$; **, $P < 0.01$; and ***, $P < 0.001$. (*B*) Whole-cell patch–clamp recordings from HEK293 cells expressing WT Kv1.2 (squares), S440A/S441A (circles), or S449A (triangles). The cells were held at −80 mV and step depolarized to +60 mV for 200 ms in +10-mV increments. Peak current amplitudes at each test potential were divided by the cell capacitance to obtain the current densities. Mean ± SE of current densities obtained (Kv1.2, $n = 11$; Kv1.2 S440A/S441A, $n = 6$; S449A, $n = 4$) were plotted against each test potential. (*C*) Dose-dependent effects on Kv1.4 surface expression in the presence of increasing amounts of WT Kv1.2, S440A/S441A, or S449A cDNA in COS-1 cells (n = three samples of 100 cells each). Symbols are the same as in *B*.

A Role for pS440/pS441 Phosphorylation in Regulating Kv1.2 Cell-Surface Expression. The data presented above suggest that pS440/pS441 phosphorylation may be acquired during intracellular trafficking of Kv1.2. To determine whether such phosphorylation affects Kv1.2 surface expression, we compared cell-surface expression of WT Kv1.2 with the S440A/S441A and S449A mutants. Cells expressing S440A/S441A and S449A exhibit a significant decrease in the number of Kv1.2-expressing cells exhibiting cell-surface Kv1.2 staining (WT Kv1.2, 17.2 ± 0.6%; S440A/S441A, 8.0 ± 1.0%; S449A, 11.6 ± 0.9%; $n = 5$, $P < 0.05$ for both mutants versus WT Kv1.2; Fig. 4*A*). Electrophysiological analyses of Kv1.2 expression levels by whole-cell patch–clamp reveal a similar pattern. HEK293 cells expressing S440A/S441A and S449A express a significantly lower level of whole-cell current than did cells expressing WT Kv1.2

(Fig. 4*B*). No differences in the macroscopic voltage-dependent activation or inactivation gating characteristics between WT and mutant channels were observed (data not shown).

Kv1.2 is typically found in mammalian brain as a component subunit of heteromeric Kv1 channel complexes (7). To investigate the effects of pS440/pS441 phosphorylation on surface expression of heteromeric Kv1 channel complexes, we expressed Kv1.4 with increasing amounts of either WT Kv1.2 or S440A/S441A and S449A mutants. As shown in ref. 12, coexpression of efficiently expressed Kv1.4 with less efficiently expressed Kv1.2 yields a modest depression in Kv1.4 cell-surface expression (Fig. 4*C*). In contrast, S440A/S441A and S449A coexpression yielded a sharp and dose-dependent decrease in cell-surface expression of Kv1.4 (Fig. 4*C*). These results suggest that regulation of Kv1.2 trafficking by phosphorylation at S440/S441 can impact trafficking of both homo- and heteromeric Kv1.2-containing Kv1 channels.

Discussion

Here we investigated the role of phosphorylation in regulating expression of Kv1.2-containing Kv channels by identifying *in vivo* phosphorylation sites on Kv1.2 in mammalian brain, showing that they correlated with Kv1.2 trafficking and that mutating these sites impacts trafficking. We identified a set of clustered sites on Kv1.2 purified from rat, human, and mouse brain (pS434, pS440, pS441, and the doubly phosphorylated pS440/pS441) and from heterologous cells (pS449). Our proteomic, biochemical, and immunocytochemical analyses show that, in heterologous cells pS440/pS441, phosphorylation is restricted to the cell-surface population of Kv1.2 channels, whereas pS449 phosphorylation is not. Moreover, mutations that directly eliminate (S440A/S441A) or indirectly interfere with (S449A) phosphorylation at pS440/pS441 negatively impact cell-surface expression of Kv1.2-containing channels. Taken together, these data support a fundamental role of phosphorylation at these sites in regulating expression levels of Kv1.2. Previous studies have shown that, in addition to trafficking determinants encoded in primary structure, reversible phosphorylation can also affect trafficking of distantly related potassium channels. This is achieved through phosphorylation-dependent suppression of an intrinsic ER retention signal on Kir1.1 (20, 21) and through generation of a 14-3-3 binding site on KCNK3 (16). Interestingly, the pS440 and pS449 sites on Kv1.2 are predicted 14-3-3 mode-1 binding sites (http://scansite.mit.edu/motifscan_seq.phtml). The role of the binding of 14-3-3 family members and other phosphorylation-dependent binding proteins in trafficking of Kv1.2 is an interesting topic for future study.

That pS434, pS440, and pS441 were found consistently phosphorylated on Kv1.2 purified from rat, human, and mouse brain suggests a common and fundamental role for these sites in different mammalian species. We note that the 40-aa region (421–460) containing these sites is absolutely conserved in all mammalian and avian Kv1.2 sequences in the nonredundant protein sequence database, and the S334, S440, S441, and S449 sites are conserved in frog and fish Kv1.2. That phosphorylation at these sites is maintained at high levels in adult rat, mouse, and human brain may suggest additional roles for such phosphorylation in regulating Kv1.2 function outside of the role in biosynthetic trafficking defined here. We should stress that phosphorylation at pS449 was distinct in that it was only observed on Kv1.2 in heterologous cells, and not in brain. However, S449 phosphorylation was less easily detected than other sites in rat brain and heterologous cell samples, and analyses of mouse and human brain did not yield coverage of the S449-containing peptide (see SI Fig. 5). That S449 phosphorylation in heterologous cells was enhanced in the ER pool and seems to be requisite for subsequent phosphorylation at the pS440/pS441 sites identified *in vivo* may imply that it is phosphorylated only transiently during Kv1.2 biosynthesis, such that it might not be well represented in adult brain, where levels of newly synthesized channels are relatively low.

Previous studies have used candidate-site approaches to identify residues critical to phosphorylation-dependent regulation of Kv1.2 expression and function. Kv1.2 currents are decreased upon Tyr kinase activation (22) through increased Kv1.2 endocytosis dependent on an intact Y132 residue in the Kv1.2 N terminus (23). As such, the Y132F mutant exhibits increased steady-state levels of Kv1.2 expression (23). Phosphorylation at S440/S441 presumably acts through a distinct mechanism, because the S440A/S441A double mutation reduces cell-surface Kv1.2 expression of both WT Kv1.2 and the Y132F mutant to a similar extent (H.V. and J.S.T., unpublished results). Tyrosine kinase activation also destabilizes Kv1.2 in the membrane by inhibiting its association with the actin-binding protein cortactin, a response dependent on an intact C-terminal Y415 and Y417 (24). A distinct N-terminal residue (T46) was found to be critical for protein kinase A-mediated enhancement of Kv1.2 currents (25), although structural studies show this residue is not surface-accessible (26). Phosphorylation at T46 and Y132 was not detected in our studies, although we obtained a robust and consistent identification of the phosphorylation sites at pS434, pS440, pS441, and pS440/pS441 in rat, mouse, and human brain, and we consistently observed unphosphorylated T46- and Y132-containing tryptic peptides. Y415 and Y417 are within a tryptic peptide that also contains the entire transmembrane S6 segment; this peptide was never observed in our MS analyses, presumably because of its overall hydrophobic nature. An inability to detect *in vivo* phosphorylation at a specific site in these whole-brain analyses of course does not preclude phosphorylation at that site in some mammalian central neurons or under conditions more closely resembling those used in the above referenced studies in heterologous cells. Moreover, our studies were limited to mammalian brain, and these sites (and others) may be present in other tissues (skeletal and smooth muscle, peripheral nervous system, etc.) that express Kv1.2.

Changes in the Kv channel phosphorylation state mediate short- and long-term changes in electrical excitability in response to altered synaptic activity, neuromodulation, and other neuronal signaling events (27). Our data suggest that signaling pathways that impact levels of Kv1.2 phosphorylation may also regulate biosynthetic trafficking of Kv1.2-containing channels. Dramatic effects of lowering functional levels of Kv1.2-containing channels by pharmacological blockade leads to enhanced depolarization-induced neurotransmitter release (1) and seizures (28), and Kv1.2 knockout mice exhibit enhanced seizure susceptibility and die on average by postnatal day 17 (8). As such, regulation of Kv1.2 activity in mammalian neurons is crucial to normal brain function. The current study suggests that stimuli that alter activity levels of Ser-directed protein kinases and phosphatases may affect expression levels of Kv1.2-containing Kv channels through effects on C-terminal Kv1.2 phosphorylation sites and biosynthetic intracellular trafficking.

Materials and Methods

Preparation of Brain Membrane Fractions and Cell Lysates. RBM or rat hippocampal membranes (RHM), mouse brain membranes (MBM), and human hippocampal or cerebellar membranes (HHM and HCM, respectively) were prepared as described in ref. 29. Human brain tissue from anonymous donors was obtained from the Brain and Tissue Bank for Developmental Disorders at the University of Maryland, Baltimore. HEK293 and COS-1 cells were cultured and lysed as described in ref. 30. Cells were transiently transfected using the Lipofectamine 2000 (Invitrogen) or Polyfect (Qiagen) reagents by following the manufacturers' protocols.

AP Treatment, Immunoblotting, Immunopurification, and Surface Biotinylation. RBM and cell lysates were incubated without or with 100 unit/ml of AP (Roche) as reported in ref. 31. Procedures for immunoblot and immunoprecipitation analysis were performed as reported in ref. 19. Mouse anti-Kv1.2 mAb (K14/16, ref. 32;

available from NeuroMab, www.neuromab.org) was used for immunoblot. For immunoprecipitation, RBM (25 mg), RHM (5 mg), MBM (10 mg), HHM (10 mg), or HCM (10 mg) were incubated with affinity-purified rabbit anti-Kv1.2C polyclonal Ab (33). Cell-surface biotinylation was performed using biotin-LC-hydrazide as described in ref. 34.

In-Gel Digestion and MS. In-gel digestion of Kv1.2 was performed in 10 ng/ml trypsin as described in ref. 19. An ultraperformance LC system (nanoACQUITY; Waters) directly coupled with an ion trap mass spectrometer (LTQ-FTl; Finnigan) was used for LC-MS/MS data acquisition. MS/MS spectra were interpreted through the Mascot searches (Matrix Science) with a mass tolerance of 20 ppm, with an MS/MS tolerance of 0.4 Da, and with phosphorylation on Ser, Thr, and Tyr residues allowed. Each filtered MS/MS spectra exhibiting possible phosphorylation was manually checked and validated. The existence of a 98-Da mass loss ($-H_3PO_4$, phosphopeptide specific CID neutral loss) and any ambiguity of phosphorylation sites were carefully examined (see *SI Materials and Methods* for details).

SILAC. HEK293 cells transiently coexpressing Kv1.2 and Kvβ2 were grown for at least five cell divisions either in normal Arg ($^{12}C_6$,$^{14}N_4$; "Arg-0") and lysine ($^{12}C_6$,$^{14}N_2$; "Lys-0") media or in isotopic Arg ($^{13}C_6$,$^{14}N_4$; "Arg-6") and Lys ($^{13}C_6$,$^{15}N_2$; "Lys-8") labeling media before harvest (19). Immunopurified Kv1.2 from both samples was subjected to SDS/PAGE and to separate excision of high and low M_r forms of Kv1.2. Portions of excised high and low bands were mixed by using amounts of the respective samples to yield similar amounts of Kv1.2 on the basis of immunoblot analyses of the immunopurified Kv1.2 pools and were subjected to in-gel digestion followed by LC-MS/MS. After database searches, relative spectral intensities were determined using Xcalibur (version 2.0) software (see *SI Materials and Methods* for details). A nonspecific/contaminant peak near the pS449 peptide peak precluded quantitation of pS449 by SILAC.

Generation of Mutant Kv1.2 α-Subunit cDNAs. Mutagenesis of recombinant rat Kv1.2 cDNA in the pRBG4 vector (35) was performed using the QuikChange site-directed mutagenesis kit (Stratagene).

Generation of Phosphospecific Abs Kv1.2P and L64/4. A synthetic peptide doubly phosphorylated at pS440/pS441 (amino acids 435–446, CPKIPpSpSPDLKK) and the nonphosphorylated equivalents were generated (Anaspec). Phosphopeptide was conjugated to keyhole limpet hemocyanin (Calbiochem) at a ratio of 1.3 mg of peptide per milligram of carrier protein by using sulfo-*m*-maleimidobenzoyl-NHS ester (Pierce) and was injected into rabbits for the production of polyclonal antisera (PRF&L). For affinity purification, the phosphorylated and nonphosphorylated peptides were conjugated to SulfoLink coupling gel (Pierce) via their terminal cysteine residue, and phosphospecific Abs were affinity-purified by a two-step affinity-purification procedure (19). MAb L64/4 was generated using standard procedures (32) from mice immunized with the same peptide. Phosphospecificity was verified by ELISA against phosphorylated and nonphosphorylated peptide coupled to BSA and by immunoblot analysis against extracts from HEK293 cells expressing Kv1.2 WT and the S440A/S441A mutant.

Immunofluorescence Staining. For surface immunofluorescence staining (14), cells were stained 48 h after transfection with ectodomain-directed rabbit polyclonal Ab Kv1.2e (13) or Kv1.4e (14) before detergent permeabilization to detect the cell-surface pool. The total cellular pool was detected by cytoplasmic-directed mAb K14/16 (Kv1.2) or K13/31 (Kv1.4) after detergent permeabilization. Alternatively, surface staining of intact cells with Kv1.2e was followed by detergent permeabilization and staining with L64/4. In other experiments, cells were fixed and permeabilized, followed by double-staining with Kv1.2P and K14/16. Bound primary Abs were detected using goat anti-mouse and anti-rabbit secondary Abs conjugated to Alexa dyes. Staining was scored under narrow-wavelength fluorescein and Texas red filter sets by using indirect immunofluorescence on a Zeiss Axioskop 2 microscope as described in ref. 30. Surface expression index (SEI) values represent the mean $\pm$ SD of expressing cells judged to be positive for surface staining as determined from at least three independent coverslips per treatment. P values < 0.05 were considered statistically significant.

Electrophysiology. Outward potassium currents were recorded at room temperature from HEK293 cells transiently expressing recombinant Kv1.2 or Kv1.2 mutants by using whole-cell voltage–clamp configuration as described in ref. 30.

We thank Lauren Guy, Michelle R. Salemi, and Dominic Siino for expert technical assistance. This work was supported by National Institutes of Health Grant NS34383 (to J.S.T.).

1. Dodson PD, Forsythe ID (2004) *Trends Neurosci* 27:210–217.
2. Coleman SK, Newcombe J, Pryke J, Dolly JO (1999) *J Neurochem* 73:849–858.
3. Rhodes KJ, Strassle BW, Monaghan MM, Bekele-Arcuri Z, Matos MF, Trimmer JS (1997) *J Neurosci* 17:8246–8258.
4. Shamotienko OG, Parcej DN, Dolly JO (1997) *Biochemistry* 36:8195–8201.
5. Stuhmer W, Ruppersberg JP, Schroter KH, Sakmann B, Stocker M, Giese KP, Perschke A, Baumann A, Pongs O (1989) *EMBO J* 8:3235–3244.
6. Ruppersberg JP, Schroter KH, Sakmann B, Stocker M, Sewing S, Pongs O (1990) *Nature* 345:535–537.
7. Trimmer JS, Rhodes KJ (2004) *Annu Rev Physiol* 66:477–519.
8. Brew HM, Gittelman JX, Silverstein RS, Hanks T, Demas VP, Robinson LC, Robbins CA, McKee-Johnson J, Chiu SY, Messing A, *et al.* (2007) *J Neurophysiol* 98:1501–1525.
9. Vacher H, Misonou H, Trimmer JS (2006) in *Protein Trafficking in Neurons*, ed Bean AJ (Elsevier, London), pp. 244–270.
10. Manganas LN, Wang Q, Scannevin RH, Antonucci DE, Rhodes KJ, Trimmer JS (2001) *Proc Natl Acad Sci USA* 98:14055–14059.
11. Li D, Takimoto K, Levitan ES (2000) *J Biol Chem* 275:11597–11602.
12. Manganas LN, Trimmer JS (2000) *J Biol Chem* 275:29685–29693.
13. Shi G, Nakahira K, Hammond S, Rhodes KJ, Schechter LE, Trimmer JS (1996) *Neuron* 16:843–852.
14. Tiffany AM, Manganas LN, Kim E, Hsueh YP, Sheng M, Trimmer JS (2000) *J Cell Biol* 148:147–158.
15. Campomanes CR, Carroll KI, Manganas LN, Hershberger ME, Gong B, Antonucci DE, Rhodes KJ, Trimmer JS (2002) *J Biol Chem* 277:8298–8305.
16. O'Kelly I, Butler MH, Zilberberg N, Goldstein SA (2002) *Cell* 111:577–588.
17. Shi G, Trimmer JS (1999) *J Membr Biol* 168:265–273.
18. Ong SE, Blagoev B, Kratchmarova I, Kristensen DB, Steen H, Pandey A, Mann M (2002) *Mol Cell Proteomics* 1:376–386.
19. Park KS, Mohapatra DP, Misonou H, Trimmer JS (2006) *Science* 313:976–979.
20. O'Connell KM, Tamkun MM (2005) *J Cell Sci* 118:2155–2166.
21. Yoo D, Fang L, Mason A, Kim BY, Welling PA (2005) *J Biol Chem* 280:35281–35289.
22. Huang XY, Morielli AD, Peralta EG (1993) *Cell* 75:1145–1156.
23. Nesti E, Everill B, Morielli AD (2004) *Mol Biol Cell* 15:4073–4088.
24. Hattan D, Nesti E, Cachero TG, Morielli AD (2002) *J Biol Chem* 277:38596–38606.
25. Huang XY, Morielli AD, Peralta EG (1994) *Proc Natl Acad Sci USA* 91:624–628.
26. Minor DL, Lin YF, Mobley BC, Avelar A, Jan YN, Jan LY, Berger JM (2000) *Cell* 102:657–670.
27. Levitan IB (1999) *Adv Second Messenger Phosphoprotein Res* 33:3–22.
28. Velluti JC, Caputi A, Macadar O (1987) *Toxicon* 25:649–657.
29. Trimmer JS (1991) *Proc Natl Acad Sci USA* 88:10764–10768.
30. Vacher H, Mohapatra DP, Misonou H, Trimmer JS (2007) *FASEB J* 21:906–914.
31. Murakoshi H, Shi G, Scannevin RH, Trimmer JS (1997) *Mol Pharmacol* 52:821–828.
32. Bekele-Arcuri Z, Matos MF, Manganas L, Strassle BW, Monaghan MM, Rhodes KJ, Trimmer JS (1996) *Neuropharmacology* 35:851–865.
33. Rhodes KJ, Keilbaugh SA, Barrezueta NX, Lopez KL, Trimmer JS (1995) *J Neurosci* 15:5360–5371.
34. Zhu J, Watanabe I, Gomez B, Thornhill WB (2001) *J Biol Chem* 276:39419–39427.
35. Nakahira K, Shi G, Rhodes KJ, Trimmer JS (1996) *J Biol Chem* 271:7084–7089.